The Journal of Experimental Biology 205, 3377–3386 (2002)
Printed in Great Britain © The Company of Biologists Limited 2002
JEB4394

Metabolite diffusion in giant muscle fibers of the spiny lobster *Panulirus argus*

Stephen T. Kinsey[1,*] and Timothy S. Moerland[2]

[1]*Department of Biological Sciences, University of North Carolina at Wilmington, 601 South College Road, Wilmington, NC 28403-5915, USA* and [2]*Department of Biological Science, Florida State University, Tallahassee, FL 32306-4370, USA*

*Author for correspondence (e-mail: kinseys@uncwil.edu)

Accepted 8 August 2002

Summary

The time- and orientation-dependence of metabolite diffusion in giant muscle fibers of the lobster *Panulirus argus* was examined using ^{31}P- and ^{1}H-pulsed-field gradient nuclear magnetic resonance. The ^{31}P resonance for arginine phosphate and the ^{1}H resonances for betaine, arginine/arginine phosphate and -CH_2/-CH groups were suitable for measurement of the apparent diffusion coefficient, *D*. Diffusion was measured axially, $D_{\parallel}$, and radially, $D_{\perp}$, in fibers over diffusion times of 20 to 300 ms. Diffusion was strongly anisotropic, and $D_{\parallel}$ was higher than $D_{\perp}$ at all times. Radial diffusion decreased with time until a steady-state value was reached at a diffusion time of ≈100 ms. Changes in $D_{\perp}$ occurred over a time scale that was consistent with previous measurements from fish and mammalian muscle, indicating that diffusion is hindered by the same types of barriers in these diverse muscle types. The time dependence indicated that the sarcoplasmic reticulum is the principal intracellular structure that inhibits mobility in an orientation-dependent manner in skeletal muscle. The abdominal muscles in *P. argus* are used for anaerobic, burst contractions during an escape maneuver. The fact that these muscle fibers have diameters that may exceed hundreds of microns in diameter, and nearly all of the mitochondria are localized near the sarcolemmal membrane, suggests that barriers that hinder radial diffusion of ATP equivalents may ultimately limit the rate of post-contractile recovery.

Key words: diffusion, giant muscle fibe, nuclear magnetic resonance, spiny lobster, *Panulirus argus*, crustacea, muscle.

Introduction

The cytoplasm is a complex and crowded medium consisting of soluble and bound macromolecules, fibrous cytoskeletal elements and membrane bound organelles (reviewed in Luby-Phelps, 1994, 2000). Intracellular diffusion of proteins and other macromolecules is significantly hindered in cells by barriers such as the cytoskeletal network (Wojcieszyn et al., 1981; Jacobson and Wojcieszyn, 1984; Luby-Phelps et al., 1987; Janson et al., 1996) and the thick and thin filament lattice in muscle cells (Jurgens et al., 1994; Arrio-Dupont et al., 1996; Papadopoulos et al., 2000). Most biochemical reactions are therefore dependent on the diffusion of small metabolites (molecular mass <1 kDa), which have diffusion coefficients (*D*) that are 2–3 orders of magnitude greater than those of proteins. In extreme cases, such as actin-rich regions of cells that exclude protein-sized macromolecules (Luby-Phelps et al., 1987), metabolic fluxes must be exclusively dependent on the diffusion of small metabolites. Therefore, the composition of intracellular barriers to diffusion and the extent to which these barriers reduce *D* of metabolites *in vivo* has important implications for our understanding of cellular energetics.

Creatine phosphate is a substrate for the enzyme creatine kinase (CK), which catalyzes the reversible transfer of a phosphoryl group from creatine phosphate to ADP, forming ATP. The time- and orientation-dependence of diffusion of creatine phosphate in skeletal muscle is of particular interest, because radial diffusion of creatine phosphate is the principal mechanism for the transport of ATP equivalents from mitochondria to the myosin ATPases in the fiber core (Mainwood and Rakusan, 1982; Meyer et al., 1984). Several groups have used pulsed-field gradient nuclear magnetic resonance (PFG-NMR) to measure non-invasively *D* of creatine phosphate in muscle cells, and *in situ D* typically has values that are 40–50 % of the bulk diffusion coefficient (D_0) of creatine phosphate in water (Moonen et al., 1990; van Gelderen et al., 1994; Hubley and Moerland, 1995; Hubley et al., 1995; Kinsey et al., 1999; de Graaf et al., 2000). The time dependence of radial ($D_{\perp}$) and axial diffusion ($D_{\parallel}$) of creatine phosphate in mammalian skeletal muscle was first measured by Moonen et al. (1990) and van Gelderen et al. (1994). These authors concluded that the time-dependent decrease in $D_{\perp}$ was a consequence of creatine phosphate being restricted within the cylindrical cell membrane (the sarcolemma), which defines the boundaries of a muscle fiber. Our own investigations of diffusion in the homogenous red and white muscles of fish revealed that the decrease in $D_{\perp}$ with time was more likely to be a result of subcellular barriers that occur on a length scale of a few μm (Kinsey et al., 1999). Candidate diffusion barriers on this length scale include the sarcoplasmic reticulum (SR) and mitochondria. Subsequent measurements by de Graaf et al. (2000) on rat skeletal muscle were interpreted to indicate that radial diffusion of creatine phosphate was restricted by undefined, cylindrical shaped structures with a diameter of 22 μm, too small to be accounted for by the sarcolemma. Therefore, while $D_{\perp}$ of creatine phosphate has been found to have a consistent pattern of time dependence in skeletal muscle, the barriers that induce the observed diffusive anisotropy are unresolved.

In the present study, we have used ^{31}P-PFG-NMR to examine the time dependence of $D_{\|}$ and $D_{\perp}$ of arginine phosphate (AP), an invertebrate phosphagen analogous to creatine phosphate, in giant fibers of spiny lobster abdominal muscle. The fibers are characterized by their extreme size, which can exceed 500 μm in diameter and 1 cm in length (Jahromi and Atwood, 1971), as well as a paucity of mitochondria, which in giant crustacean fibers are almost exclusively localized to the periphery of the cell (subsarcolemmal mitochondria; Kent and Govind, 1981; Tse et al., 1983). The large size of the fibers means that aerobic post-contractile recovery involves diffusion of arginine phosphate over hundreds of μm, and barriers to diffusion may ultimately limit this process. Use of giant fibers in the present study minimizes the effect of restriction within the cylindrical sarcolemma, allowing an examination of intracellular barriers. In addition, the lack of intermyofibrillar mitochondria means that the contractile filaments and SR are the only obvious anisotropic barriers to diffusion. We also used ^{1}H-PFG-NMR to examine diffusion of protonated metabolites, which differ from AP in their molecular mass and chemical characteristics. We tested the hypotheses that (i) all of the metabolites would have similar anisotropic diffusion, (ii) the time dependence of radial diffusion would be consistent with hindrance by μm-scale structural barriers such as the SR, and (iii) diffusion coefficients collected at long diffusion times (i.e. distance-averaged over intracellular barriers) would be inversely proportional to molecular mass, as expected in an isotropic solution.

Materials and methods

Specimens

Adult spiny lobsters *Panulirus argus* Latreille were obtained from the Keys Marine Laboratory in Long Key, FL, USA or from the University of Florida Marine Laboratory in St Augustine, FL, USA. Specimens were maintained at 22°C in 1000 l tanks containing recirculating seawater. Lobsters were exposed to a 12 h:12 h light:dark cycle and fed frozen shrimp daily.

NMR procedures

Muscle fibers were prepared as described in Kinsey and Ellington (1996). Lobsters were placed on ice for 20 min prior to dissection. The carapace on the dorsal surface of the abdomen was removed, and bundles of 2–3 giant fibers were isolated from the deep extensor abdominal muscle. The muscle fibers were tied at either end with 6–0 surgical silk and suspended in the center of a 1.9 mm i.d. glass capillary superfusion chamber housed in a NMR probe. The glass capillary chamber was connected at either end to superfusion lines that were fed through the bottom of the probe to a pair of peristaltic pumps. The fibers were continuously superfused at a flow rate of 10 ml min^{-1} with lobster saline solution (457 mmol l^{-1} NaCl, 15 mmol l^{-1} KCl, 1.8 mmol l^{-1} $MgCl_2$ and 2.5 mmol l^{-1} $MgSO_4$, buffered with 10 mmol l^{-1} Hepes and 10 mmol l^{-1} MES, pH 7.5). The temperature of the superfused tissue was maintained at 20°C using a refrigerated recirculating water bath. The NMR probe had a horizontal, five-turn solenoidal radiofrequency coil (2.6 mm i.d.) tunable to ^{1}H and ^{31}P, which surrounded the superfusion chamber.

Experiments were performed on a Bruker 600 MHz DMX wide-bore spectrometer with micro-imaging gradient coils (960 mT m^{-1} maximum gradient strength) located at the National High Magnetic Field Laboratory in Tallahassee, FL, USA. Data were acquired and processed using a Silicon Graphics Indigo workstation and Bruker X-Win NMR software. The probe was oriented so that the long axis of the superfusion chamber, and hence the long axis of the muscle fibers, was oriented parallel to the *y*-axis imaging gradient. Therefore, both the *x* and the *z* gradients was oriented perpendicular to the muscle fibers. This careful alignment of the probe and the homogeneous orientation of the giant fibers within the probe ensured that our measurements of axial diffusion (along the *y*-axis) and radial diffusion (along the *x*- or *z*-axis) contained essentially no contamination from fibers oriented at angles off-axis. To measure *D* of phosphorylated compounds, ^{31}P-spectra were acquired at 242 MHz using a bipolar gradient pulse-stimulated echo sequence, with a longitudinal eddy current delay (BPP-LED; Cotts et al., 1989; Wu et al., 1995; Gibbs, 1997) as previously applied to fish muscle fibers (Kinsey et al., 1999). This sequence minimizes both eddy-current-induced artifacts and the background gradients generated from susceptibility contrast in heterogenous samples (Fordham et al., 1996). To measure *D* of protonated compounds, ^{1}H-spectra were collected at 600 MHz using the BPP-LED pulse sequence as above modified to include the CHESS (*CHE*mical *S*hift *S*elective) water suppression sequences (Moonen et al., 1990) inserted during the relaxation delay and during the mixing time (Fig. 1). The CHESS sequences are as described in Kinsey and Ellington (1996). In an isotropic solution, the NMR peak amplitude, *A*, is described by:

$$\ln(A/A_0) = -(\gamma G\delta/2\pi)^2(\Delta - \delta/3 - \tau/2)D = -bD\,, \qquad (1)$$

where A_0 is the peak amplitude in the absence of diffusion-weighting gradients. The magnitude of the motion-encoding

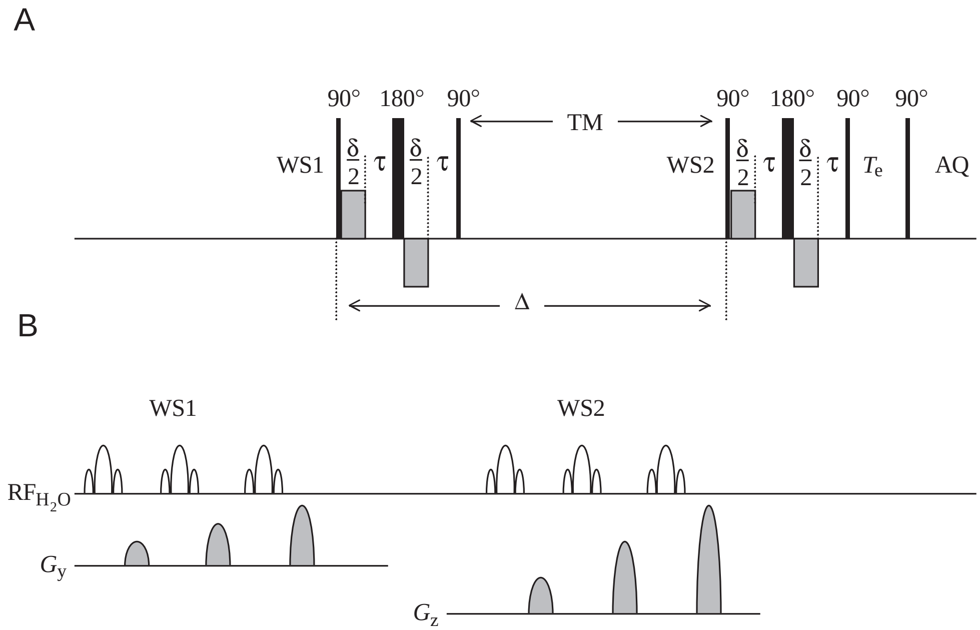

Fig. 1. (A) Pulse sequence used to measure $D_{\parallel}$ and $D_{\perp}$ in lobster abdominal muscle fibers. The solid bars represent excitatory radiofrequency pulses, with the magnetization tip angle (degrees) indicated over each pulse. The stippled bars represent magnetic field gradient pulses. TM is the mixing time, T_e, echo time, δ is the duration of the spatial-encoding gradients, τ is a short delay, Δ is the approximate diffusion time (corrected as described in text), AQ is the signal acquisition period, and WS1 and WS2 are water suppression sequences that were used in the ^{1}H spectra only. (B) The water suppression sequences are shown diagrammatically (for details, see Kinsey and Ellington, 1996). Diffusion coefficients at a given diffusion time were determined by collecting a series of spectra at different amplitudes of the spatial-encoding gradients. The diffusion time was adjusted by changing the value of Δ. Additional details are given in the text.

wave vector, $\gamma G\delta/2\pi$, is defined by the magnetogyric ratio of ^{31}P or ^{1}H, γ, the gradient amplitude *G* and the gradient duration of each bipolar pair δ. The diffusion time is defined by the term $\Delta-\delta/3-\tau/2$, where Δ is the time between the leading edges of each gradient pair, and τ is the time between the end of each gradient and the next radiofrequency pulse (Fig. 1). *b* is the composite diffusion-weighting factor.

To measure *D*, a series of spectra were collected with different values for *G*. In all experiments, δ was 2 ms, τ was 250 µs, the recycle time was 2 s, the eddy current delay was 20 ms and spectra were collected in either 256 or 512 scans. Gradient strengths ranged from 100 to 960 mT m^{-1}, and the current pulses through the gradient coils were pre-emphasized so that the magnetic field gradient produced was square, as shown in Fig. 1A. At least four data points with different values of *G* were collected for each diffusion measurement. Diffusion was measured at seven diffusion times, which ranged from 20 to 300 ms. The diffusion time was adjusted by changing Δ values, while all other time variables were constant. The direction in which diffusion was measured was alternated for each diffusion time (e.g. $D_{\perp}$ was measured at 20 ms followed by measurement of $D_{\parallel}$ at 20 ms). Several determinations of *D* could be made for each fiber preparation.

Analysis

The time dependence of intracellular diffusion coefficients is influenced by fixed structures in the cytoplasm, and the highly organized structure of muscle would be expected to have a different effect on $D_{\perp}$ and $D_{\parallel}$. ATP equivalents must diffuse from subsarcolemmal mitochondria to the fiber core, so barriers to radial diffusion directly impact cellular energy transport. Several dominant structural barriers are likely to affect radial diffusion, such as: (i) the nm-scale myofilament lattice, which consists primarily of the filamentous contractile proteins actin and myosin, (ii) µm-scale subcellular membranes, which in lobster abdominal muscle principally constitute the SR, and (iii) the 1×10^2 µm-scale sarcolemmal membrane, which is the cylindrical membrane that delineates individual muscle cells. Two of these barriers, the myofilament lattice and the sarcolemmal membrane, both have known dimensions and their effect on radial diffusion can be predicted.

We have previously used a volume-averaging approach (Carbonell and Whitaker, 1984) to model the time dependence of $D_{\perp}$ in the myofilament lattice, and details of this procedure are available in Kinsey et al. (1999). The effect of restriction within the cylindrical sarcolemma on the time dependence of diffusion has been approximated by Gibbs (1997), by interpolating between the theoretical long- and short-time asymptotic behavior of $D_{\perp}$ to yield:

$$D_{\perp}/D_0 = \left[1 + \frac{4}{3\sqrt{\pi}}\sqrt{D_0\Delta/a^2} - 1.81(D_0\Delta/a^2)^{0.81} + 4(D_0\Delta/a^2)\right]^{-1}, \quad (2)$$

where *a* is the radius of the cylinder (muscle fiber). It is expected that diffusion through the SR would yield a curve of $D_{\perp}$ against diffusion time that is similar in shape to that for diffusion through the myofilament lattice. However, while we know that the SR membranes have radial increments on the µm scale, we lack an adequate morphometric description of the reticulations in lobster muscle SR to mathematically describe the effect on $D_{\perp}$. Therefore, we can analyze the effect of the

SR by elimination, since its influence on $D_{\perp}$ will have a time dependence that is intermediate to that of the myofilament lattice and the sarcolemmal membrane (Kinsey et al., 1999).

Results

The lobster muscle fibers could be maintained in an energetically favorable condition for >6 h, based on the constant amplitudes of the ^{31}P-NMR peaks arising from arginine phosphate, ATP and P_i, as well as the lack of change in intracellular pH, determined by the chemical shift of the P_i peak (reviewed in Kinsey and Moerland, 1999). The only phosphorylated compound with sufficient signal for measuring *D* at all diffusion times was arginine phosphate, although we were able to reliably measure ATP diffusion in some cases (see below). Peak assignments in ^{1}H-spectra were made by spiking muscle extracts with putative compounds and by comparison of our spectra to the chemical shift data given in Agar et al. (1991). The betaine peak at 3.2 p.p.m. was large and well resolved in ^{1}H-NMR spectra, and *D* could be measured at all diffusion times for this metabolite (Fig. 2). Although several other peaks were also visible, the extremely small tissue sample yielded relatively little signal for the smaller peaks at the high gradient strengths necessary to measure *D*. In addition, most of the other peaks in ^{1}H-spectra from lobster muscle contain contributions from multiple metabolites, thus confounding measurement of *D*. However, two additional peaks did demonstrate sufficient signal and linear amplitude attenuation with increasing gradient strength, and *D* could be measured for these peaks at some diffusion times. A peak at 1.95 p.p.m., which principally comprises arginine, but may have a slight contribution from lysine, could be measured at diffusion times ranging from 30 to 150 ms. Although this peak has a chemical shift specific to arginine, most of this amino acid is probably in the form of arginine phosphate, which facilitates comparison of the ^{31}P- and ^{1}H-NMR methods. Diffusion of a small peak at 1.0 p.p.m. was also measured at diffusion times ranging from 30 to 150 ms. We do not have an identity for this peak, but it likely consists of -CH and -CH_2 groups of aliphatic amino acids. Despite the uncertainty in assignment of this peak, it was included because it has diffusion coefficients that are consistent with a low molecular mass solute, and because it further illustrates the general diffusive pattern in muscle (see below). Several sizeable peaks with chemical shifts of 3.0 to 4.0 p.p.m. are present in Fig. 2, but were not included in the analysis because they were often reduced or absent in other ^{1}H-spectra.

Those peaks that were examined always had linear decreases in signal amplitude as *G* was increased at all of the diffusion times that were analyzed. Fig. 3 illustrates this linearity as well as the characteristic difference in attenuation slopes associated with axial and radial diffusion. The time dependence of $D_{\|}$ and $D_{\perp}$ is presented in Fig. 4. The unrestricted, bulk diffusion coefficient D_0 of a metabolite in water would be expected to be higher than *D* in the crowded environment inside a muscle fiber. D_0 of arginine phosphate has been previously determined to be 4.05×10^{-6} cm^2 s^{-1} (Ellington and Kinsey, 1998), which is considerably higher than the *D* values for arginine phosphate in lobster muscle (Fig. 4A). The most obvious pattern in both the ^{31}P- and ^{1}H-NMR derived data was the orientation-dependence of diffusion within lobster muscle fibers, where $D_{\perp}$ was lower than $D_{\|}$ at all diffusion times for all of the metabolites (Fig. 4). From 20 to 100 ms, a substantial reduction in $D_{\perp}$ was apparent for arginine phosphate and for betaine. This pattern was not resolved for the two small ^{1}H resonances arising from arginine/arginine phosphate and -CH/-CH_2 groups since we were unable to measure *D* at the shortest diffusion times. In contrast to the pattern for radial diffusion, $D_{\|}$ was only slightly time-dependent for all of the compounds and demonstrated no

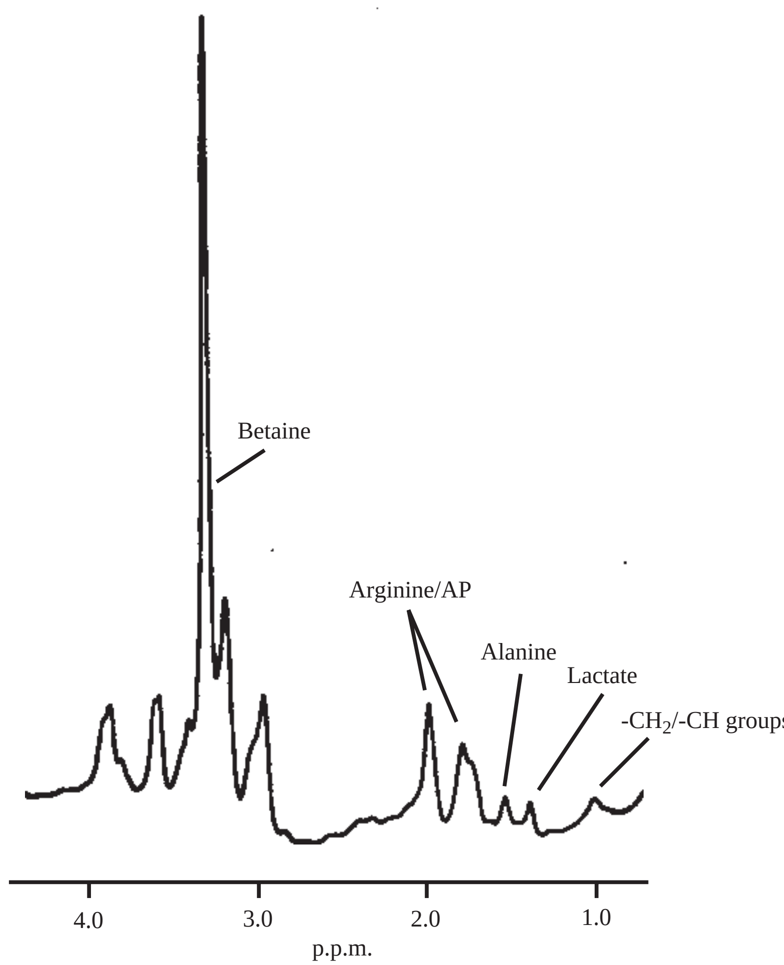

Fig. 2. A region of a lobster abdominal muscle ^{1}H-spectrum. The peaks for betaine, arginine/arginine phosphate (at 1.95 p.p.m.) and -CH_2/-CH groups yielded linear attenuation plots and sufficient signal-to-noise ratios to allow measurement of *D* at several diffusion times. Alanine and lactate methyl peaks are also indicated for reference, although diffusion of these metabolites was not examined in the present study.

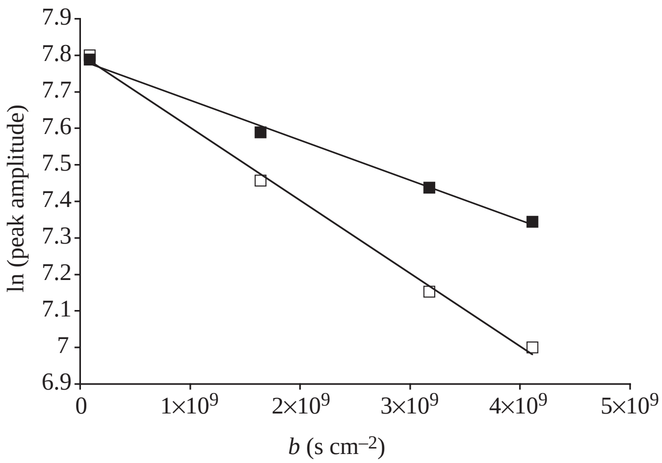

Fig. 3. Typical attenuation plot of the NMR peak amplitude as a function of the diffusion-weighting factor *b* in the axial (open squares) and radial (filled squares) directions in *P. argus* muscle. This example is from a measurement of arginine phosphate diffusion at a diffusion time of 150 ms. A steeper attenuation slope is indicative of a higher *D*, as seen for axial diffusion.

rapid decrease at short diffusion times. The *D* values in both orientations were fairly stable after about 100 ms, as would be expected for diffusion through a porous medium.

Since radial diffusion of arginine phosphate from subsarcolemmal mitochondria to the fiber interior is important in aerobic post-contraction recovery in lobster fibers, it is of interest to examine the effect of intracellular barriers on the net movement of arginine phosphate. Fig. 5 shows the extent to which the radial root-mean-square (RMS) displacement of arginine phosphate in lobster muscle deviates from that of arginine phosphate in a non-restricted environment. At the maximal diffusion time of 300 ms measured in this study, arginine phosphate diffused a distance of only 7 μm, whereas in an unrestricted environment, it would diffuse twice that distance.

The principal cause of the diffusive anisotropy can be inferred from the model data presented in Fig. 6, which predicts the effects of the myofilament lattice and the sarcolemmal membrane on the normalized radial diffusion coefficient of arginine phosphate ($D_{\perp}/D_0$). The results of this analysis would be nearly identical for the other metabolites. The predicted effect of the nm-scale myofilament lattice leads to a very rapid reduction in $D_{\perp}/D_0$ (<0.2 ms), after which a steady-state diffusion coefficient is reached (Fig. 6A). In contrast, restriction of metabolites within the 300 μm diameter sarcolemma of lobster fibers only minimally impacts radial diffusion (Fig. 6B). In fact, $D_{\perp}$ is only about 5% less than D_0 at a diffusion time of 300 ms (Fig. 6B). It is expected that the rate of decay of $D_{\perp}/D_0$ with time will be considerably less in the large fibers of lobsters than in cells of ‘normal’ dimensions. In Fig. 6C the combined effect of these two types of structural features has been removed from the arginine phosphate $D_{\perp}$

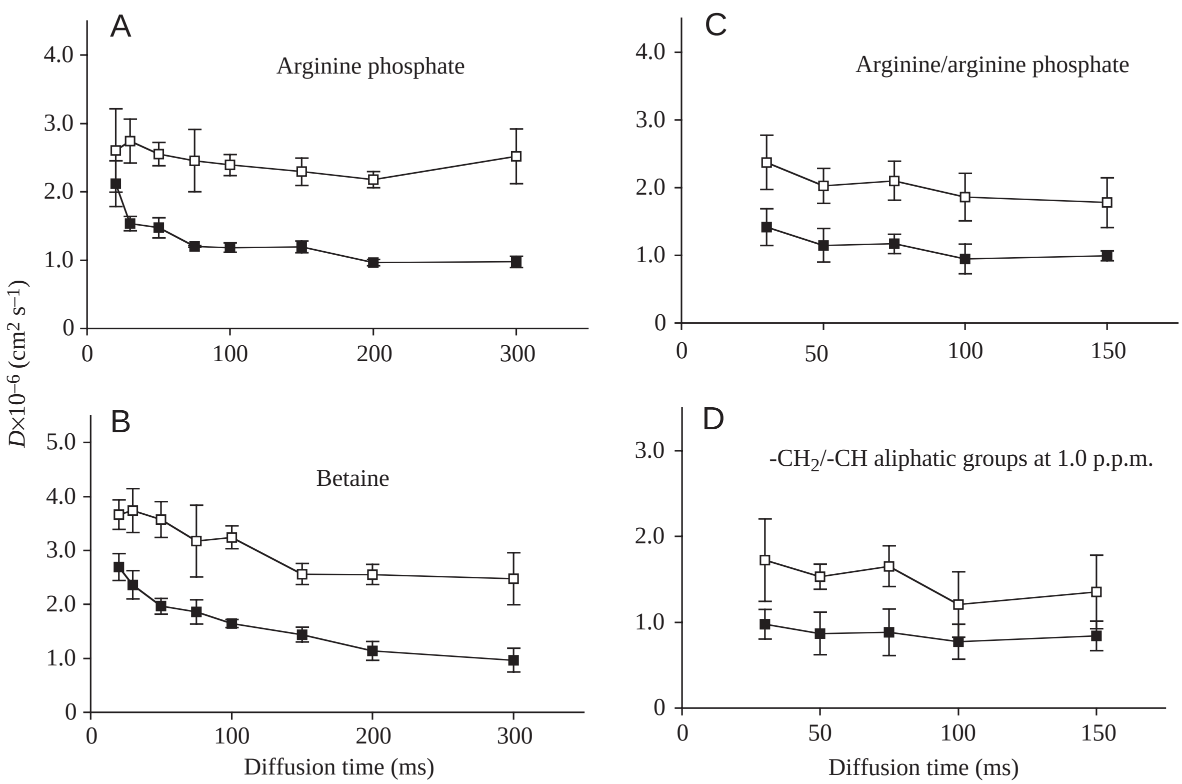

Fig. 4. Time dependence of $D_{\parallel}$ (open squares) and $D_{\perp}$ (closed squares) for several metabolites in abdominal muscle fibers of *P. argus*. Diffusion was measured using the ^{31}P-NMR peak for arginine phosphate (A), and the ^{1}H-NMR peaks arising from (B) betaine, (C) arginine/arginine phosphate and (D) -CH_2/-CH groups. Values are means ± S.E.M. (*N*=4, except for -CH_2/-CH peak, where *N*=3).

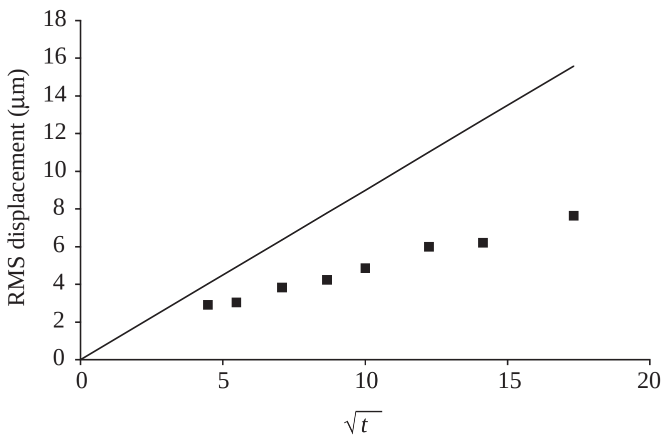

Fig. 5. The radial root-mean-square (RMS) displacement of arginine phosphate in *P. argus* fibers as a function of the square root of the diffusion time. The RMS displacement λ is described by $\lambda=\sqrt{2Dt}$, where t is the diffusion time (ms). The unrestricted RMS displacement was calculated using a D value for AP of $4.054\times10^{-6}\,cm^2\,s^{-1}$ (Ellington and Kinsey, 1998). The effect of restriction is noted by the deviation of the radial RMS displacement values of AP in the fibers (filled squares) from the line depicting the time-dependent displacement in an unrestricted medium. Data points were calculated from the mean values of $D_{\perp}$ shown in Fig. 4A.

values, and compared to the bulk diffusion coefficient for arginine phosphate ($4.05\times10^{-6}\,cm^2\,s^{-1}$). Here, the residual time dependence of AP $D_{\perp}$ values presumably is caused by structures other than the myofibrillar lattice or the sarcolemmal membrane.

Fig. 7 shows the relationship between intracellular D values and the reciprocal of the square root of molecular mass. This relationship should be linear in an isotropic solution, as well as in a porous medium at long diffusion times (i.e. when D reaches a steady state). We examined $D_{\|}$ values at a diffusion time of 100 ms. This selection was made, not only because the D values have largely stabilized at this point, but also because measurements of $D_{\|}$ at a diffusion time of 100 ms are available for lactate and alanine in lobster abdominal muscle fibers (Kinsey and Ellington, 1996), and these data can be included in the analysis. In addition, we were able to estimate $D_{\|}$ of ATP by averaging values from three diffusion times collected from a muscle preparation that yielded an adequate signal-to-noise ratio and linear attenuation plots. We arrived at a steady-state value of $D_{\|}$ (100–300 ms diffusion time) of $1.13\pm0.23\,cm^2\,s^{-1}$ (N=3), which is consistent with previous measurements of ATP diffusion in skeletal muscle (de Graaf et al., 2000). The long-time behavior of $D_{\|}$ can be seen to be linearly related to the square root of molecular mass (Fig. 7).

Discussion

The principal finding of the present study was that metabolite diffusion was anisotropic in *P. argus* muscle fibers (Fig. 4). In addition to the orientation-dependence that was apparent for all metabolites, a rapid decrease in $D_{\perp}$ was observed at the short diffusion times that could be measured for arginine phosphate (^{31}P experiments) and betaine (^{1}H experiments). ^{31}P-PFG–NMR methods have been used extensively in studies of creatine phosphate and ATP diffusion, and the results from different laboratories using a variety of tissues yield similar values for D (Yoshizaki et al., 1990; Hubley et al., 1995; Hubley and Moerland, 1995; de Graaf et al., 2000) and patterns of D time dependence (Moonen et al., 1990; van Gelderen et al., 1994; Kinsey et al., 1999; de Graaf et al., 2000). ^{1}H-PFG–NMR has been applied to measure metabolite diffusion in skeletal muscle (de Graaf et al., 2001), but ^{1}H-spectra of *P. argus* muscle have predominantly small peaks that overlap considerably and complicate measurements of D. An exception is betaine, which has an unusually large peak amplitude that minimizes the effect of overlap with other peaks. The facts that the time-dependent pattern of $D_{\perp}$ for betaine closely matches that for AP (Fig. 4), and that both ^{31}P- and ^{1}H-derived measurements yield D values that are linearly dependent on $\sqrt{M_r}^{-1}$ (Fig. 7), suggest that the ^{1}H-PFG–NMR method employed here yields reliable results. As noted earlier, the -CH/-CH_2 and arginine/arginine phosphate resonances probably yield D values that are a composite of several metabolites. However, the compelling feature of the metabolites that give rise to these two small peaks is their anisotropic diffusive behavior, which is consistent with that observed for the well-resolved peaks of AP and betaine.

Several previous studies have focused on diffusion of the phosphagen, creatine phosphate, in skeletal muscle, because of its role in cellular energy transport (Meyer et al., 1984; Walliman et al., 1992). The invertebrate phosphagen, arginine phosphate, fulfils the same role in crustacean muscle and is responsible for the vast majority of high-energy phosphate flux (Ellington and Kinsey, 1998). We will therefore focus on arginine phosphate in the present discussion. An important feature of our data is that the time dependence of arginine phosphate diffusion was nearly identical to that previously observed for creatine phosphate diffusion in white muscle fibers from cold-acclimated goldfish *Carasius auratus* (Kinsey et al., 1999). In this previous work, as in the present study, we used small tissue samples and carefully oriented the fibers axially along the *y*-imaging gradient in order to measure $D_{\|}$ or $D_{\perp}$. In both fish white muscle and *P. argus* muscle, $D_{\|}$ of the phosphagen (creatine phosphate or arginine phosphate) was essentially independent of time over the range of diffusion times measured (Fig. 4A). However, we know that $D_{\|}$ must decrease in a time-dependent fashion prior to our earliest measurements to account for the fact that $D_{\|}<D_0$. Similarly, the time course over which phosphagen $D_{\perp}$ was reduced was the same in fish white muscle and *P. argus* muscle. In both types of muscle, $D_{\perp}$ reached a fairly constant value at a diffusion time of 75–100 ms (Fig. 4A). The nearly identical patterns of $D_{\perp}$ of creatine phosphate and arginine phosphate in fish white muscle and *P. argus* muscle, respectively, suggest that the barriers that restrict diffusion are the same in both tissues. White muscle fibers from goldfish that have been acclimated to cold have an extensive SR and

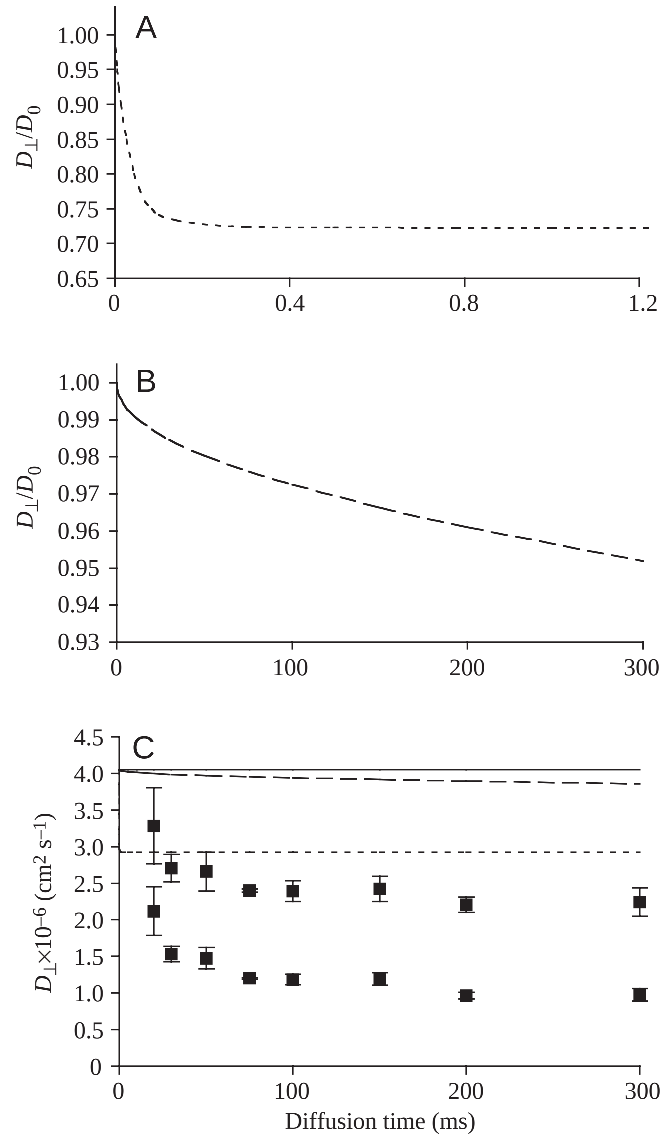

Fig. 6. The predicted effect of the thick and thin filament lattice and restriction within the cylindrical sarcolemma on the time dependence of $D_{\perp}$ for arginine phosphate. (A) The effect of the nm-scale thick and thin filament lattice, using a porosity of 0.86, on the relative $D_{\perp}$ of arginine phosphate. Note the short time required for $D_{\perp}$ to reach a steady-state value. (B) The effect of restriction within the sarcolemmal membrane of a cell with a radius of 150 µm on the relative $D_{\perp}$ of arginine phosphate (note: axes are different than A). (C) The predicted time dependence of the absolute $D_{\perp}$ of arginine phosphate in an unrestricted environment (solid line), in the presence of the thick and thin filament lattice (dotted line), and when restricted within the sarcolemmal membrane of a cell with a radius of 150 µm (dashed line). The lower squares depict the raw data collected for $D_{\perp}$ of arginine phosphate (Fig. 4A), and the upper squares show the predicted $D_{\perp}$ of arginine phosphate if the effects of the thick and thin filament lattice and restriction within the sarcolemma are removed. The upper squares therefore predict the pattern of $D_{\perp}$ time dependence imposed by residual, µm-scale barriers. See text for additional details.

relatively few core (intermyofibrillar) mitochondria (Tyler and Sidell, 1984). Giant glycolytic fibers from crustaceans also have an extensive SR, and are virtually devoid of intermyofibrillar mitochondria (S. T. Kinsey, unpublished results; Jahromi and Atwood, 1969; Tse et al., 1983). Therefore, with respect to diffusion barriers, the principal difference between the two types of muscle fibers is the fiber size. White muscle fibers from goldfish are approximately 100 µm in diameter (Kinsey et al., 1999), while *P. argus* fibers used in the present study were approximately 300 µm in diameter. The fact that the time dependence of $D_{\perp}$ was identical in these two fibers of dramatically different sizes indicates that restriction by the sarcolemmal membrane cannot account for the observed reduction in $D_{\perp}$.

Other studies have found a time-dependent decrease in D of creatine phosphate in mammalian skeletal muscle that is similar to that observed in the present paper, but the interpretations have been quite different (Moonen et al., 1990; van Gelderen et al., 1994; de Graaf, 2000). In rat quadriceps muscle *in vivo*, apparent limits to creatine phosphate displacement at long diffusion times indicated a compartment with an axial dimension of 44 µm, which the authors suggested corresponded to the length of a muscle fiber (Moonen et al., 1990). These diffusion measurements were made on muscles that were oriented at an angle relative to the diffusion-weighting gradients, and D was measured in only one direction. Subsequently, van Gelderen et al. (1994) examined the time dependence of diffusion in rabbit skeletal muscle *in vivo* along the x, y and z axes of the laboratory frame (the muscle fibers were not oriented with respect to these axes). The orientation- and time-dependent values of D were used to calculate the trace of the diffusion coefficient (D_{Tr}), assuming restriction within a cylindrical compartment. D_{Tr} is invariant to orientation, which is sometimes important in *in vivo* experiments where orientation of fibers may not be controllable or when fiber orientation is not uniform. From the time-dependent pattern of D_{Tr}, van Gelderen et al. (1994) estimated that the cell diameter of rabbit skeletal muscle was 17 µm. De Graaf et al. (2000) recently conducted a similar analysis of the time dependence of D_{Tr}, also fitted to a cylindrical model, in rat skeletal muscle *in vivo*. These authors estimated that cylindrical compartments with diameters of 16 and 22 µm restricted the motion of ATP and creatine phosphate, respectively. However, de Graaf et al. (2000) recognized that these dimensions were considerably smaller than the dimensions of rat skeletal muscle cells, and they concluded that yet-to-be-defined, subcellular, cylindrical barriers restrict ATP and creatine phosphate diffusion in skeletal muscle.

In contrast to the conclusions drawn from studies of diffusion in mammalian skeletal muscle, we believe that the principal barrier that induces the anisotropy observed in PFG–NMR measurements is the reticulated SR membrane. Several lines of evidence support this conclusion. First, our modeling results clearly indicate that the time-dependent reduction in diffusive flux through the nm-scale thick and thin

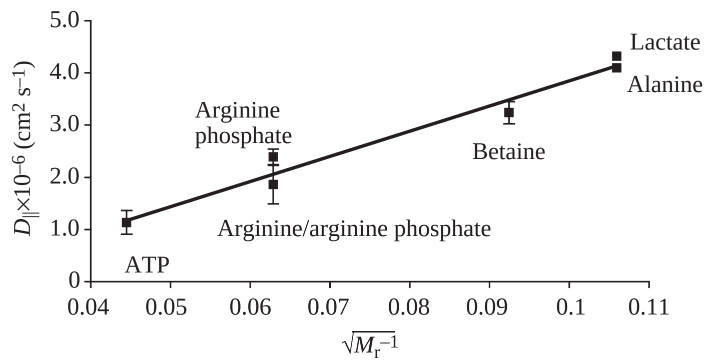

Fig. 7. The relationship between $D_{\|}$ at a diffusion time of 100 ms and the reciprocal of the square root of the relative molecular mass M_r. The arginine phosphate and ATP D values were collected using ^{31}P-NMR, while the values for betaine and arginine/arginine phosphate were collected using ^{1}H-NMR. The D values for lactate and alanine are from Kinsey and Ellington (1996). See text for additional details.

filament lattice is too rapid to be detected by NMR methods (Fig. 6A). This intuitively satisfying result is very robust to moderate variation in the estimate of myofilament porosity or filament dimensions. Second, restriction within a cylinder the size of most skeletal muscle fibers has only a slight effect on the observed time dependence of $D_{\perp}$ (Fig. 6B) (Gibbs, 1997; Kinsey et al., 1999). This was partly what motivated us to select crustacean giant muscle fibers for this study, since at physiologically relevant diffusion times the effect of the sarcolemma on $D_{\perp}$ is virtually undetectable. This leaves us with intracellular barriers with length scales intermediate between the myofilament lattice, which has a nm-length scale, and the sarcolemma, which has a 1×10^2 µm-length scale. In lobster giant muscle fibers, the only obvious barrier is the SR membrane, and the associated sarcolemmal invaginations, or clefts, that are peculiar to crustaceans (Peachey, 1967; Selverston, 1967). The SR is a reticulated membrane envelope that wraps around each myofibril or a bundle of 2–3 myofibrils. Each myofibril is ≈1 µm in diameter, so the cylindrical partial membrane of the SR would serve as a strong barrier to radial diffusion, but would not be expected to hinder axial diffusion. The sarcolemmal clefts in crustaceans are partial membranes that project radially into the fiber core with a linear spacing of approximately 50 µm (Peachey, 1967; Selverston, 1967). These membranous structures would therefore be expected to have some effect on radial, but not axial, diffusion in crustacean muscle. Whereas the SR will constitute a similar barrier to radial diffusion in crustacean, fish and mammalian skeletal muscle, the sarcolemmal clefts are specific to crustaceans. However, the sarcolemmal clefts are an incomplete membrane with relatively large linear spacing, and the effect of this potential barrier on radial diffusion is likely to be minimal.

As described above, de Graaf et al. (2000) have proposed an alternative view of the subcellular structures that induce diffusive anisotropy in skeletal muscle. However, we know of no cylindrical barriers in skeletal muscle that have a length scale of 16–22 µm as described in their study (de Graaf et al., 2000). We contend that their determination of a length scale of this magnitude is derived from the fact that these authors fit their diffusion data to a model of restriction within an impermeable cylinder. Thus, while their method of determining D_{Tr} has great utility when fiber orientation cannot be controlled, we do not believe it yields relevant length scales of barriers to diffusion.

Part of the difficulty in assessing the effect of the SR (and sarcolemmal clefts) is the complex three-dimensional structure of these membranes. For instance, we know that diffusion through the SR will lead to a time-dependent reduction in $D_{\perp}$ until a steady-state value is reached, as is the case for diffusion through the thick and thin filament lattice (Fig. 6A). However, the effect of the SR on diffusion will be a function of *two* variables, neither of which are adequately described or easily modeled. Both the membrane porosity and the length scale in the direction of diffusion will have an impact on the time dependence of $D_{\perp}$. Because of this complication, our conclusions are drawn from the fact that barriers in muscle fibers from mammals, fish and crustaceans induce the same time-dependent anisotropy despite the fact that they are dramatically different with respect to cell size, mitochondrial density, and the presence or absence of sarcolemmal clefts. All of these tissues have in common a well-developed SR, however, and the function of this organelle in Ca^{2+} dynamics demands that its radial length scale is relatively invariant, regardless of the type of skeletal muscle.

Another finding of the present study is that when the effect of the thick and thin filament lattice and restriction within the sarcolemma are mathematically removed, the intracellular D values at short diffusion times do not differ substantially from D_0 (Fig. 6C). This is in agreement with previous studies, which indicated that at short diffusion times the cytoplasm viscosity was not significantly higher than that of water (Luby-Phelps et al., 1993; van Gelderen et al., 1994; de Graaf et al., 2000). In addition, the steady-state diffusion of metabolites in *P. argus* muscle had diffusion coefficients that were inversely proportional to their molecular mass (Fig. 7). This is consistent with the idea that when diffusion is temporally (and hence spatially) averaged across intracellular structural barriers, the cytoplasmic space in lobster abdominal muscle behaves as would be expected for a well-mixed, bulk solution.

Diffusion analyses such as the present study are useful for probing the nature of the intracellular environment, but they also raise the following question: does the diffusive flux of metabolites impose constraints on muscle function? The abdominal muscles in lobsters, crayfish and shrimp are used solely for a rapid series of 'tail-flips' that propel the animal away from potential predators at a high velocity. The abdominal muscle bundles are composed almost exclusively of fast-twitch, glycolytic fibers. These fast-twitch fibers of lobsters and crabs tend to be the largest, often exceeding 500 μm in diameter and more than 1 cm in length (Jahromi and Atwood, 1971; Tse et al., 1983). In addition, nearly all of the mitochondria in these fibers are located peripherally near the sarcolemmal membrane (subsarcolemmal mitochondria; Kent and Govind, 1981; Tse et al., 1983). This arrangement of mitochondria forms a cylinder of aerobic metabolic potential that has essentially the same dimensions as the muscle fibers themselves. There are important functional implications to the combination of extreme cellular dimensions and highly localized aerobic machinery. Rapid, aerobically powered contraction is logically forbidden, since this would require rapid diffusive flux of ATP-equivalents (i.e. arginine phosphate) over a distance of hundreds of microns. The displacement of molecules *via* diffusion, λ, scales as the square-root of the diffusion time, t: $\lambda=\sqrt{2Dt}$. The steady-state value of D for arginine phosphate *in situ* is $\approx 1\times10^{-6}\,\mathrm{cm^2\,s^{-1}}$ (Fig. 5), meaning that it takes several minutes for arginine phosphate to diffuse from subsarcolemmal mitochondria at the fiber periphery, to the sites of ATP demand at the fiber core of a crustacean giant muscle fiber. In contrast, muscle that contracts aerobically has relevant diffusion distances that can be traversed in milliseconds. Since the escape-response in lobsters is induced by a short-term burst of muscle activity (England and Baldwin, 1983), reliance on anaerobic metabolism (phosphagen hydrolysis and glycolysis) to supply ATP poses no obvious problems. However, post-contractile recovery ultimately relies on aerobic metabolism, and the large dimensions of crustacean fibers and barriers to radial diffusive flux would be expected to severely limit the rates of these processes.

The metabolic restrictions imposed by extreme diffusion distances are apparent in the pattern of post-exercise recovery in crustacean fast-twitch muscles, which differs substantially from the mammalian paradigm. An early phase of recovery is the resynthesis of phosphagen and restoration of ionic gradients across membranes, which allows a second round of high-force contractions. In mammalian skeletal muscle, creatine phosphate is rapidly resynthesized by aerobic processes (Kushmerick, 1983; Meyer, 1988). In crustacean muscle, however, AP stores are replenished *via* anaerobic glyogenolysis (Ellington, 1983; Kamp, 1989), presumably because the large diffusion distances and barriers to diffusive flux make aerobic recovery unacceptably slow. The aerobic phase of recovery in crustaceans that follows includes the resynthesis of glycogen, processing of lactate and restoration of muscle pH, and these processes occur over a protracted time course of several hours (Milligan et al., 1990; Henry et al., 1994). Whether the combination of extreme distances and hindered diffusion in giant fibers is the proximate cause for the slow recovery process is not known. Other properties, such as metabolic potential and oxygen supply, may ultimately limit aerobic metabolism. In this scenario, excessive diffusion distances would not be limiting *per se*, but would simply not be selected against. However, it is clear that the large diffusion distances and barriers to diffusion impose severe limits on the rate of post-contractile recovery, even if aerobic metabolic potential and oxygen supply were increased. This argument also raises issues as to the nature of the SR in fast-contracting, aerobic fibers. Here, a substantial SR is required for rapid excitation–contraction coupling, but it must be sufficiently permeable to permit high rates of ATP-equivalent flux from mitochondria to the myosin ATPase.

In summary, metabolite diffusion in lobster giant muscle fibers is anisotropic, indicating that the barriers to radial diffusion are more substantial than those that hinder axial diffusion. The similarity of the time dependence of $D_{\perp}$ in crustacean muscle to that found in skeletal muscle from mammals and fish suggests a common diffusive barrier, despite the fact that these tissues differ dramatically in fiber diameter and mitochondrial density. The time-dependent reduction in $D_{\perp}$ is consistent with barriers on a μm scale, and the most likely candidate is the SR membrane system. The combination of large diffusion distances and barriers to diffusive flux appear to severely limit the capacity for aerobic metabolic processes in crustacean giant muscle fibers.

The authors gratefully acknowledge many useful discussions with Dr Bruce R. Locke and Dr Stephen Gibbs. We thank the National High Magnetic Field Laboratory, Tallahassee, FL, USA for the use of NMR instrumentation. We also appreciate the help of Dr William F. Herrnkind with animal supply and maintenance. This work was supported by grants from the National Institutes of Health (R15-AR46184-01A1) to S.T.K. and the National Science Foundation (DBI-99-78613) to S.T.K. and (IBN-98-08120) to T.S.M.

References

Agar, N. S., Rae, C. D., Chapman, B. E. and Kuchel, P. W. (1991). ^{1}H-NMR spectroscopic survey of plasma and erythrocytes from selected marsupials and domestic animals of Australia. *Comp. Biochem. Physiol.* **99B**, 575-597.

Arrio-Dupont, M., Cribier, S., Foucault, G., Devaux, P. F. and d'Albis, A. (1996). Diffusion of fluorescently labeled macromolecules in cultured muscle cells. *Biophys. J.* **70**, 2327-2332.

Carbonell, R. G. and Whitaker, S. (1984). Heat and Mass Transfer in Porous Media. In *Fundamentals of Transport Phenomena in Porous Media* (ed. J. Bear and M. Y. Corapcioglu), pp. 121-198. Dordrecht: Martinus Nijhoff Publishers.

Cotts, R. M., Hoch, M. J. R., Sun, T. and Marker, J. T. (1989). Pulsed field gradient stimulated echo methods for improved NMR diffusion measurements in heterogenous systems. *J. Magn. Reson.* **83**, 252-262.

de Graaf, R. A., van Kranenburg, A. and Nicolay, K. (2000). *In vivo* ^{31}P-NMR diffusion spectroscopy of ATP and phosphocreatine in rat skeletal muscle. *Biophys. J.* **78**, 1657-1664.

de Graaf, R. A., Braun, K. P. J. and Nicolay, K. (2001). Single-shot diffusion trace ^{1}H-NMR spectroscopy. *Magn. Reson. Med.* **45**, 741-748.

Ellington, W. R. (1983). The recovery from anaerobic metabolism in invertebrates *J. Exp. Zool.* **228**, 431-444.

Ellington, W. R. and Kinsey, S. T. (1998). Energy transport in primitive spermatozoa. *Biol. Bull*. **195**, 264-272.

England, W. R. and Baldwin, J. (1983). Anaerobic energy metabolism in the tail musculature of the Australian Yabby *Cherax destructor* (Crustacea, Decapoda, Parastacidae): role of phosphagens and anaerobic glycolysis during escape behavior. *Physiol. Zool.* **56**, 614-622.

Fordham, E. J., Mitra, P. P. and Latour, L. L. (1996). Effective diffusion times in multiple-pulse PFG diffusion measurements in porous media. *J. Magn. Reson.* **121A**, 187-192.
Gibbs, S. J. (1997). Observations of diffusive diffraction in a cylindrical pore by PFG–NMR. *J. Magn. Res.* **124**, 223-226.
Henry, R. P., Booth, C. E., Lallier, F. H., and Walsh, P. J. (1994). Post-exercise lactate production and metabolism in three species of aquatic and terrestrial decapod crustaceans. *J. Exp. Biol.* **186**, 215-234.
Hubley, M. J. and Moerland, T. S. (1995). Application of homonuclear decoupling to measures of diffusion in biological ^{31}P-spin echo spectra. *NMR Biomed.* **8**, 113-117.
Hubley, M. J., Rosanske, R. C. and Moerland, T. S. (1995). Diffusion coefficients of ATP and creatine phosphate in isolated muscle: pulsed gradient ^{31}P-NMR of small biological samples. *NMR Biomed.* **8**, 72-78.
Jacobson, K. A. and Wojcieszyn, J. W. (1984). The translational mobility of substances within the cytoplasmic matrix. *Proc. Natl. Acad. Sci. USA* **81**, 6747-6751.
Jahromi, S. S. and Atwood, H. L. (1971). Structural and contractile properties of lobster leg-muscle fibers. *J. Exp. Zool.* **176**, 475-486.
Janson, L. W., Ragsdale, K. and Luby-Phelps, K. (1996). Mechanism of size cutoff for steric exclusion from actin-rich cytoplasmic domains. *Biophys. J.* **71**, 1228-1234.
Jürgens, K. D., Peters, T. and Gros, G. (1994). Diffusivity of myoglobin in intact skeletal muscle cells. *Proc. Natl. Acad. Sci. USA* **91**, 3829-3833.
Kamp, G. (1989). Glycogenolysis during recovery from muscular work. *Biol. Chem.* **370**, 565-573.
Kent, K. S. and Govind, C. K. (1981). Two types of tonic fibers in lobster muscle based on enzyme histochemistry. *J. Exp. Zool.* **215**, 113-116.
Kinsey, S. T. and Ellington, W. R. (1996). ^{1}H- and ^{31}P-nuclear magnetic resonance studies of L-lactate transport in isolated muscle fibers from the spiny lobster *Panulirus argus*. *J. Exp. Biol.* **199**, 2225-2234.
Kinsey, S. T., Penke, B., Locke, B. L. and Moerland, T. S. (1999). Diffusional anisotropy is induced by subcellular barriers in skeletal muscle. *NMR Biomed*. **11**, 1-7.
Kinsey, S. T. and Moerland, T. S. (1999). The use of NMR for examining intracellular pH in living systems. In *Regulation of Tissue pH in Plants and Animals: A Reappraisal of Current Techniques* (ed. E. W. Taylor, S. Egginton and J. A. Raven), pp. 45-67. Cambridge: Cambridge University Press.
Kushmerick, M. J. (1983). Energetics of muscle contraction. In *Handbook of Physiology*, Section 10, *Skeletal Muscle* (ed. L. Peachey, R. Adrian and S. R. Geiger), pp. 189-236. Bethesda, Maryland: American Physiological Society.
Luby-Phelps, K., Castle, P. E., Taylor, D. L. and Lanni, F. (1987). Hindered diffusion of inert tracer particles in the cytoplasm of mouse 3T3 cells. *Proc. Natl. Acad. Sci. USA* **84**, 4910-4913.
Luby-Phelps, K., Mujumdar, S., Mujumdar, R., Ernst, L., Galbraith, W. and Waggoner, A. (1993). A novel fluorescence ratiometric method confirms the low solvent viscosity of the cytoplasm. *Biophys. J.* **65**, 236-242.
Luby-Phelps, K. (1994). Physical properties of cytoplasm. *Curr. Opin. Cell Biol.* **6**, 3-9.
Luby-Phelps, K. (2000). Cytoarchitecture and physical properties of the cytoplasm: volume, viscosity, diffusion, intracellular surface area. *Int. Rev. Cytol.* **192**, 189-221.
Mainwood, G. W. and Rakusan, K. (1982). A model for intracellular energy transport. *Can. J. Physiol. Pharmacol*. **60**, 98-102.
Meyer, R. A., Sweeney, H. L., and Kushmerick, M. J. (1984). A simple analysis of the 'phosphocreatine shuttle'. *Am. J. Physiol.* **246**, C365-C377.
Meyer, R. A. (1988). A linear model of muscle respiration explains monoexponential phosphocreatine changes. *Am. J. Physiol.* **257**, C1149-C1157.
Milligan, C. L., Walsh, P. J., Booth, C. E., and McDonald, D. G. (1989). Intracellular acid–base regulation during recovery from locomotor activity in the blue crab (*Callinectes sapidus*). *Physiol. Zool.* **62**, 621-638.
Moonen, C. T. W., van Zijl, P. C. M., Le Bihan, D. and DesPres, D. (1990). *In vivo* NMR diffusion spectroscopy: ^{31}P application to phosphorus metabolites in muscle. *Magn. Reson. Med.* **13**, 467-477.
Papadopoulos, S., Jürgens, K. D. and Gros, G. (2000). Protein diffusion in living skeletal muscle fibers: dependence on protein size, fiber type, and contraction. *Biophys. J.* **79**, 2084-2094.
Peachey, L. D. (1967). Membrane systems of crab fibers. *Am. Zool.* **7**, 505-513.
Selverston, A. (1967). Structure and function of the transverse tubular system in crustacean muscle fibers. *Am. Zool.* **7**, 515-525.
Tse, F. W., Govind, C. K. and Atwood, H. L. (1983). Diverse fiber composition of swimming muscles of the blue crab, *Callinectes sapidus*. *Can. J. Zool.* **61**, 52-59.
Tyler, S. and Sidell, B. D. (1984). Changes in mitochondrial distribution and diffusion distances in muscle of goldfish upon acclimation to warm and cold temperatures. *J. Exp. Zool.* **232**, 1-9.
van Gelderen, P., DesPres, D., van Zijl, P. C. M. and Moonen, C. T. W. (1994). Evaluation of restricted diffusion in cylinders. Phosphocreatine in rabbit leg muscle. *J. Magn. Reson.* **103B,** 255-260.
Walliman, T. M., Wyss, M., Brdiczka, D., Nicolay, K., and Eppenberger, H. M. (1992). Intracellular compartmentation, structure and function of creatine kinase isoenzymes in tissues with high fluctuating energy demands: the 'phosphocreatine circuit' for cellular energy homeostasis. *Biochem. J.* **281**, 21-40.
Wojcieszyn, J. W., Schlegel, R. A., Wu, E.-S. and Jacobson, K. A. (1981). Diffusion of injected macromolecules within the cytoplasm of living cells. *Proc. Natl. Acad. Sci. USA* **78**, 4407-4410.
Wu, D., Chen, A. and Johnson, C. S., Jr (1995). An improved diffusion-ordered spectroscopy experiment incorporating bipolar-gradient pulses. *J. Magn. Reson.* **115A**, 260-264.
Yoshizaki, K., Watari, H. and Radda, G. K. (1990). Role of phosphocreatine in energy transport in skeletal muscle of bullfrog studied by ^{31}P-NMR. *Biochim. Biophys. Acta*. **1051**, 144-150.